Polym. Bull. (2013) 70:1819–1833
DOI 10.1007/s00289-013-0927-y

ORIGINAL PAPER

Synthesis and characterization of polyurethane/titanium dioxide nanocomposites obtained by in situ polymerization

Vinícius Demétrio da Silva · Leonardo M. dos Santos · Suelen M. Subda · Rosane Ligabue · Marcus Seferin · Carlos L. P. Carone · Sandra Einloft

Received: 16 October 2012 / Revised: 8 January 2013 / Accepted: 26 January 2013 /
Published online: 5 February 2013

Abstract The development of new polymeric and polymeric based materials is fundamental to meet the market demands. This work aims the synthesis and characterization of polyurethane/titanium dioxide nanocomposite, using low cost commercial raw materials. Nanocomposites were synthesized by in situ polymerization reactions in which titanium dioxide were added in the following proportions, by weight, in relation to the mass obtained from the pure polymer: 0.5, 1.0, 2.0, 3.0, 5.0, 7.0, and 10.0 %. These reactions were based in poli (ε-caprolactone) and 1,6-diisocyanatohexane. The materials were characterized by infrared spectroscopy Fourier transform, scanning electron microscopy, differential scanning calorimetry analysis, thermogravimetric analysis, dynamic mechanical thermal analysis, and UV–Vis spectroscopy. Based on the obtained results it was concluded that the nanocomposites synthesized by in situ polymerization presented, in general, thermal properties (degradation temperature) and mechanical properties higher than the pure polymer.

Keywords Nanocomposites · Polyurethane · In situ polymerization

V. Demétrio da Silva · L. M. dos Santos · R. Ligabue · M. Seferin · C. L. P. Carone · S. Einloft (✉)
Programa de Pós-Graduação em Engenharia e Tecnologia de Materiais (PGETEMA)—PUCRS, Pontifícia Universidade Católica do Rio Grande do Sul—PUCRS, Porto Alegre, Brazil
e-mail: einloft@pucrs.br

S. M. Subda · R. Ligabue · M. Seferin · C. L. P. Carone · S. Einloft
Faculdade de Química (FAQUI)—PUCRS, Pontifícia Universidade Católica do Rio Grande do Sul—PUCRS, Porto Alegre, Brazil

S. M. Subda · M. Seferin
Programa de Educação Tutorial (PET-Química)—PUCRS, Pontifícia Universidade Católica do Rio Grande do Sul—PUCRS, Porto Alegre, Brazil

Introduction

Polyurethanes (PUs) are one of the most versatile and used polymeric materials. It has several applications, such as, flexible foam in upholstered furniture, rigid foam insulation in walls, PU thermoplastic devices used in medical equipment, footwear, coatings, adhesives, sealants, flooring and car interiors, among others [1]. Its mechanical, thermal, and chemical properties can be modified by the reaction between a wide range of polyols and polyisocyanates [2].

On the other hand, the polymeric nanocomposites are a class of materials in which the polymer matrix is filled with particles (fillers or reinforcements) where at least one of its dimensions is in the nanometer range. These nanocomposites typically exhibit superior thermomechanical performances and barrier properties to gases and liquids, even with a small amount of filler added to the matrix, as well as improvements in rigidity when compared to the virgin polymer [3]. An increase in the degradation of nanocomposites of biodegradable polymer matrix was also noticed [4]. The maximization of the properties in nanocomposites is due to the drastic increase in the contact surface between the fillers and the polymeric matrices when compared to conventional microcomposites [5–7].

For the production of polymer nanocomposites, there are three known methods: by extrusion of the polymeric matrix with the nanofiller; by solubilizing the polymer in a solvent followed by the addition of the filler; and by in situ polymerization, which was the first method used to synthesize the nanocomposite polymer/clay. In this technique, the monomer migrates between the layers of the silicate, so the polymerization reaction may occur between the layers interleaved, after the exfoliation of the clay [8]. In the case of TiO_2, the in situ polymerization occurs around the TiO_2 nanoparticles [9].

The choice of the filler is based on the composite application and desired properties, as well as in the cost. Several types of fillers could be added to different polymeric matrices. The materials used in the nanocomposites production could be of an organic/organic, inorganic/inorganic, or inorganic/organic nature [10]. Among the most extensively studied and used fillers, the carbonates, being calcium carbonate ($CaCO_3$) the more widely used [11], metal oxides (Al_2O_3, Fe_2O_3, TiO_2 and ZnO), clay, and silica-alumina could be cited [12]. $CaCO_3$ is widely used for the nanocomposites production, probably due to its natural abundance and low cost. But it is common to find in the literature problems related to the $CaCO_3$ dispersion into the polymer matrix [13]. Titanium dioxide (TiO_2) nanoparticles are widely used in the industry, and their properties are a function of the crystal structure, size, and particle morphology [12, 14]. TiO_2 applications can range from anti-corrosion, self-cleaning coatings, inks in solar cells to photocatalysts. Nanostructured materials with TiO_2 include spheroidal nanoparticles, nanotubes, nanosheets, and nanofibers. Only in the late 1990's, TiO_2 nanotubes began to be synthesized [15].

There is a growing interest in the developing of nanocomposites composed of organic polymers and TiO_2 nanoparticles. This is based on perceived positive features in these nanocomposites, such as mechanical, dielectric, and thermal properties [16].

Polymer/TiO_2 composites were produced with various polymer matrices, such as polycarbonate [17], polypyrrole [18], epoxy resins [19], polyester [20], polyacrylate

[21], poly (methyl methacrylate) [22], polyimide [23, 24], polystyrene [25], polyaniline [26], and PU [27–31].

So, in this scenario, this work aimed to obtain PU nanocomposites by in situ polymerization, using TiO_2 (without any pre-treatment) as nanofiller.

Experimental

The synthesis of nanocomposites were performed from the reaction between poly (caprolactone) diol (PCL, MM = 2,000 g/mol, Sigma-Aldrich) and 1,6-diisocyanatohexane (HDI, for synthesis, Merck) in the NCO/OH molar ratio of 1:1. Dibutyl tin dilaurate (Miracema-Nuodex Ind.) was used as catalyst (0.1 % w/w); methyl ethyl ketone (P.A., Merck) was used as solvent (about 50 mL). TiO_2 (Merck) was added in the beginning of the reactions at the proportions of 0.5, 1.0, 2.0, 3.0, 5.0, 7.0, and 10.0 % by weight relative to the yield of the pure polymer. Through SEM analysis and "Image Tool"^{TM} software the particle size distribution of the TiO_2 employed was assessed. The particles showed an average diameter of 164 nm, with a deviation of 33 nm.

The reactions were performed in a glass reactor of 500 mL with five inputs, in which a mechanical stirring, a thermocouple for temperature control (40 °C) reflux system, and an addition funnel were coupled. The reactions were carried out in one step and conducted under N_2 atmosphere. The system was kept at reflux for a reaction time of 2 h 30 min. The reactions were followed by Fourier transform infrared spectroscopy (FTIR—PerkinElmer FTIR spectrometer model Spectrum100). Differential scanning calorimetry (DSC) (TA Instruments model Q20 equipment) was used to measure the material's melting temperature (T_m) and crystallization temperature (T_c). The DSC analyses were performed in two cycles, only the second cycle was used to collect the data. The materials were also analyzed by thermogravimetric analysis (TGA) (TA Instruments Model SDT Q600) and dynamic mechanical thermal analysis (DMTA) (TA Instruments Model Q800 equipment) for thermo-mechanical tests. Stress/strain tests were carried out, at 25 °C, with rectangular shape films measuring thickness close to 0.15 mm, length 12 mm, and a width of approximately 7.0 mm. The Young moduli of the materials were determined according to ASTM D638. The analyses were carried out in triplicate. For assessment of the size and distribution of the fillers in the polymer matrix the scanning electron microscopy (SEM) mode backscattered electrons (BSE) aided by X-ray spectrometer for scattered energy was used. An UV–Vis spectrophotometer (PerkinElmer Instruments-Lambda 35) in a wavelength of 200–700 nm was employed to evaluate the composites. All samples were prepared in the form of films with a thickness of 0.10 mm approximately.

Results and discussion

The PU reactions were conducted by in situ polymerization by the reaction of PCL and HDI. TiO_2 nanoparticles were added at the beginning of the reaction as described in the experimental section.

The pure PU, the TiO_2, and the nanocomposites were characterized by infrared spectroscopy. The assignment of the bands were done in relation to the values of characteristic frequencies for the groups existing in the materials according to the literature [27, 29, 32].

Figure 1a shows the FTIR spectrum of TiO_2 in which it is possible to visualize the presence of a band at 3,430 cm^{-1} and another at 1,635 cm^{-1} assigned to hydroxyl groups on the TiO_2 surface. The bands at 700, 643, and 550 cm^{-1} are characteristic for the anatase crystalline form [32] of TiO_2. Figure 1c shows the spectrum of the pure PU, where it is possible to see a band in the region of 3,444 and 3,385 cm^{-1} corresponding to the NH groups of the urethane bonds. The wave numbers of 2,939 and 2,864 cm^{-1} are assigned to different vibrational modes of the CH_2 group. The band at 1,727 cm^{-1} is characteristic of the C=O group of the urethane bond. The region of 1,528 cm^{-1} shows characteristic bands for CN and NH bonds of the urethane groups. The group CO–O can be identified by the presence of a band in 1,235 cm^{-1}. In the regions of 1096, 1065, and 1,042 cm^{-1} bands corresponding to the presence of the N–CO–O and COC groups are observed. A band in the region of 1,159 cm^{-1} corresponding to COC segment present at the flexible segment in the polymer chain was also observed (Fig. 1c).

In Fig. 1b a change in the 700–550 cm^{-1} range (characteristic band of the TiO_2) in the composite spectrum, indicating the addition of TiO_2 in the PU matrix is visible. The disappearance of the hydroxyl bands formerly present onto the TiO_2

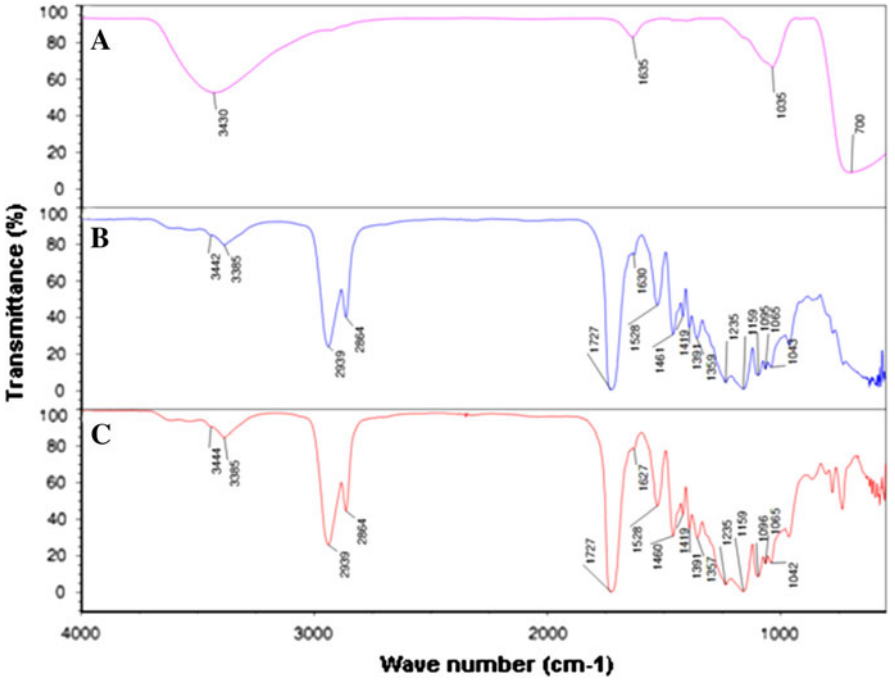

Fig. 1 IR spectra in **a** TiO_2 commercial, **b** PU/10 % TiO_2, and **c** pure PU

surface was also observed. According to the literature [27], and by infrared analysis (Fig. 1a), the commercial TiO_2 has hydroxyl groups on its surface. These OH groups could compete with the diol hydroxyl groups, during the polymerization, reducing the yield of the reaction as well as they can interact with the carbonyl groups of the urethane bond changing the nanocomposites properties. The reaction of the OH of the TiO_2 and ZnO was reported [33, 34] leading to the changes in the nanocomposites properties.

In order to confirm the reactivity of TiO_2 with HDI, a reaction was carried out between them in the same reaction conditions used in the synthesis of the compounds, without any PCL addition to the reactor. Figure 2 presents the FTIR spectra of TiO_2 (A), the product of the reaction (B) and HDI (C). In Fig. 2b, the typical bands for TiO_2 and HDI, as well as, the absence of the band of the group N=C=O (2,261 cm^{-1}) and the formation of a new band at 3,324 cm^{-1} assigned to the NH bond indicating the reaction between TiO_2 and HDI can be seen. Besides that, the band of 1,625 cm^{-1} in the product could be attributed to the carbonyl group of the urethane bond formed.

It was possible to see in the IR spectra details, Fig. 3, that the hydroxyl groups of the TiO_2 interact with urethane bond, by observing the NH stretching zone, around 1,528 cm^{-1} and around 3,380 cm^{-1}. One can observe a decreasing in the intensity of the bands when it was used until 2 wt% of TiO_2, this behavior was reported for nanocomposites PU/TiO_2 with addition of the filler until 0.42 wt% and attributed to the more favorable formation of hydrogen bonds between the hard segments and the

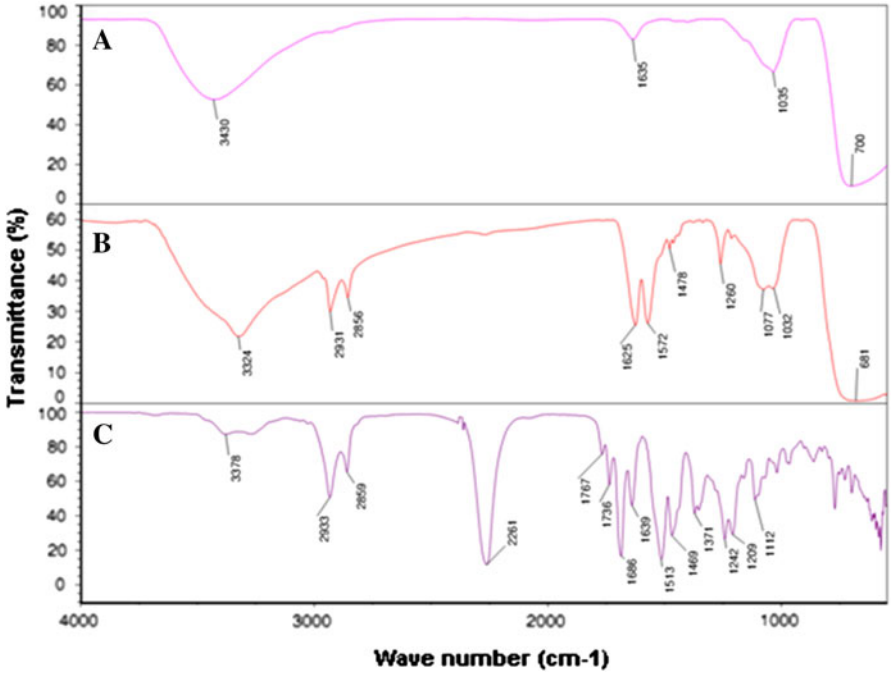

Fig. 2 IR spectra in **a** TiO_2, **b** the product of the reaction HDI/TiO_2 and **c** HDI

filler instead of the interaction of the hard and soft segments [34]. Increasing the amount of the filler above 2 % the effect was the inverse, probably due to the increase in the interaction filler/filler in relation to the interaction filler/polymer.

The GPC analysis corroborated the infrared results, showing that when the amount of TiO_2 has increased into the polymeric matrix, the numeric average molecular weight (M_n) and weight average molecular weight (M_w) have decreased.

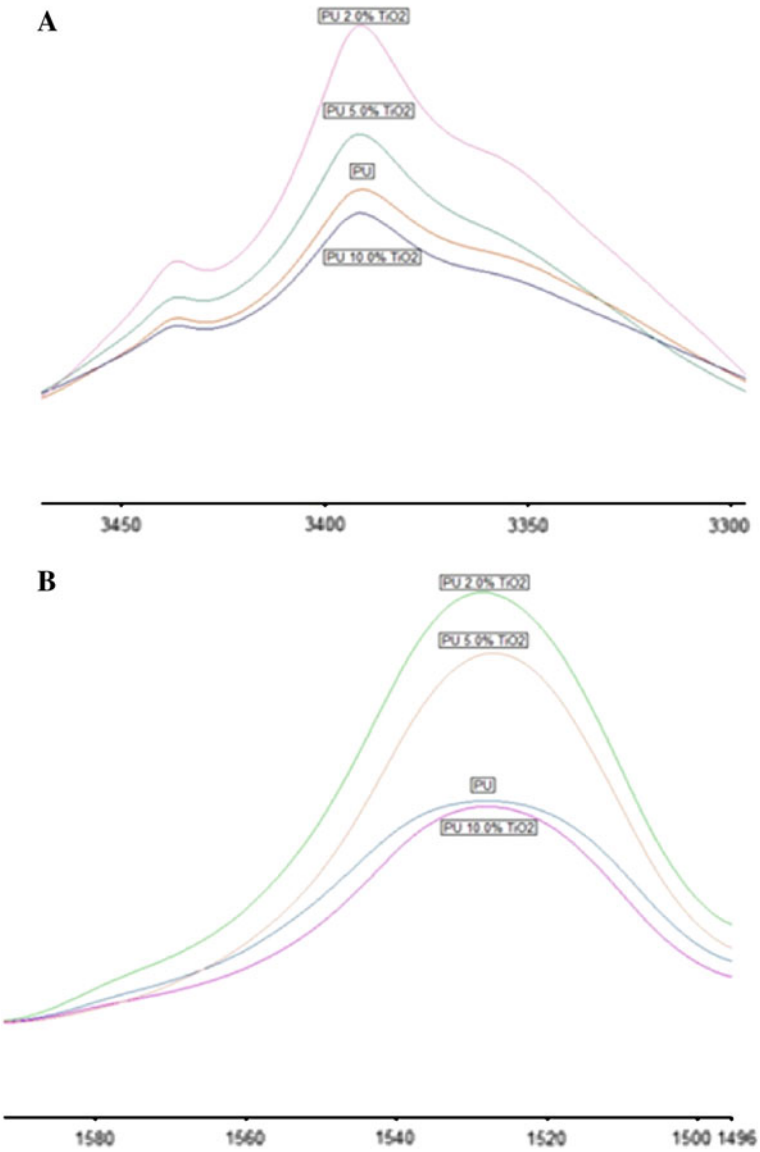

Fig. 3 FTIR absorbance spectra for the characteristic polyurethane bands, NH stretching vibrations [3,380 cm^{-1} (**a**) and 1,528 cm^{-1} (**b**)]. The peaks are normalized and the baseline corrected

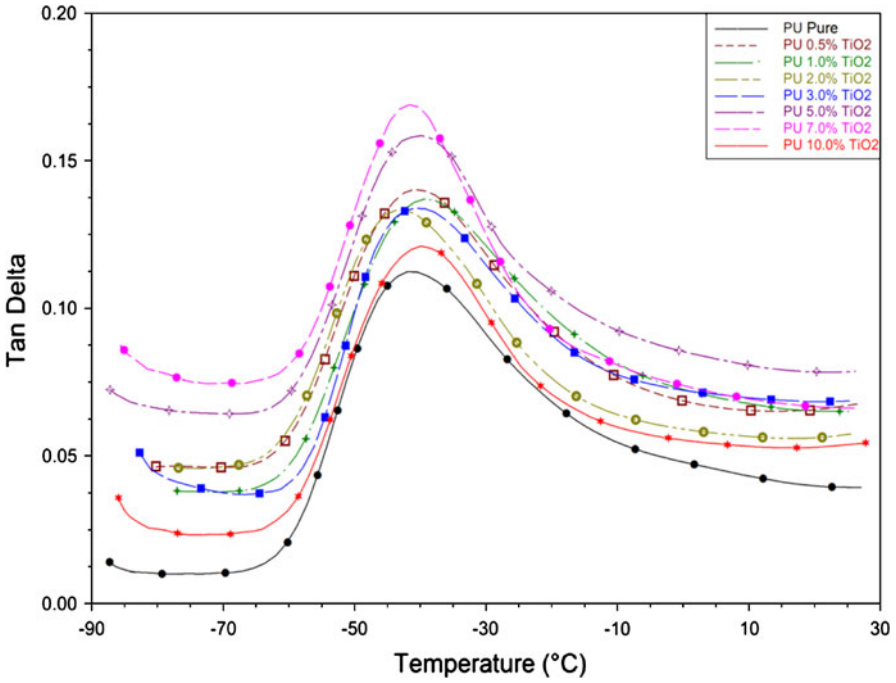

Fig. 4 DMTA curves for the T_g of nanocomposites synthesized with 0.0, 0.5, 1.0, 2.0, 3.0, 5.0, 7.0, and 10.0 % TiO_2

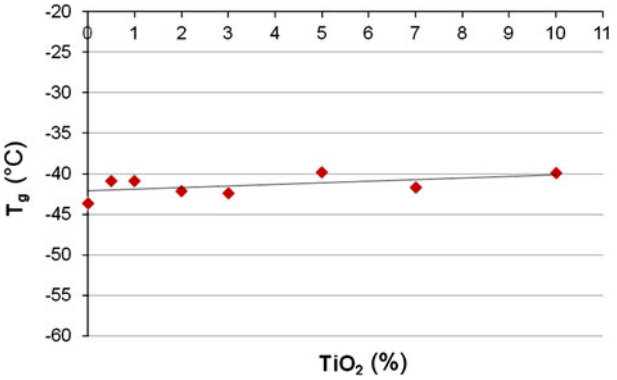

Fig. 5 Relationship between T_g of the nanocomposites and TiO_2 amount (0.0, 0.5, 1.0, 2.0, 3.0, 5.0, 7.0, and 10.0 %)

The numeric molecular weight values varied from M_n 40,000 Da for PU to M_n 30,000 Da in the composite with 10 % of filler, and the weight average molecular weight varied from M_w 75,000 Da to PU to M_w 50,000 Da for the composite (10 % of filler).

This behavior may be associated to the presence of OH groups on the filler surface (as seen in the infrared analysis). The hydroxyl groups of the TiO_2 compete

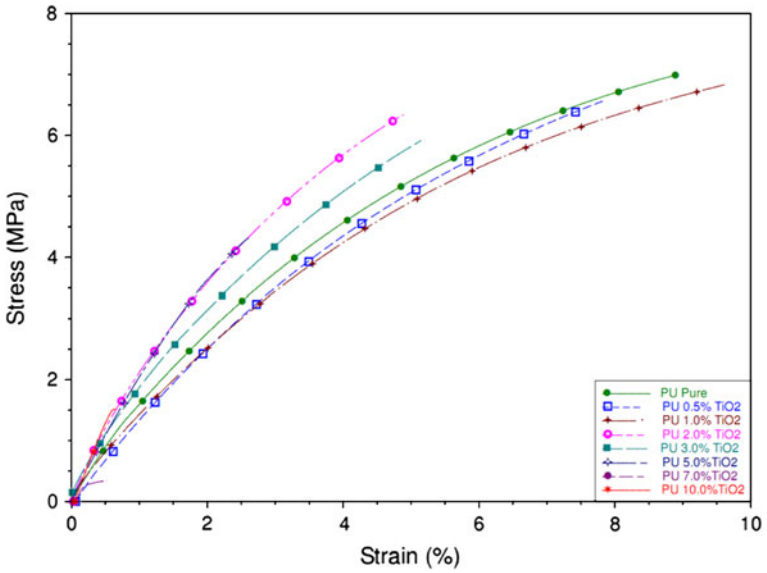

Fig. 6 Stress × Strain, by DMA, of PUs formed with 0.0; 0.5; 1.0; 2.0; 3.0; 5.0; 7.0; and 10.0 % of TiO_2

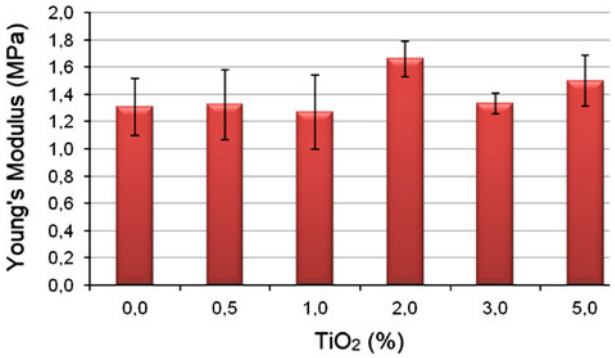

Fig. 7 Young's modulus values for nanocomposites synthesized with 0.0, 0.5, 1.0, 2.0, 3.0, and 5.0 % TiO_2

with the hydroxyl groups of the PCL diol, lowering the polymerization yield, resulting in smaller polymer chains when compared to the pure polymer.

The DSC analysis showed no significant changes in the T_c and T_m of the material synthesized with the addition of TiO_2 in relation to the pure polymer.

The sensitivity of the analysis by DMTA is approximately three orders of magnitude higher than that of a conventional thermal analysis technique as, for example, DSC [35]. In this way, the high Tanδ peak was adopted as the T_g peak (Fig. 7). The material with the lowest T_g was the pure polymer (approximately −44 °C), and the highest T_g was obtained by addition of 5.0 and 10.0 % TiO_2 (approximately −40 °C for both materials) (Fig. 8). The slight increase in the T_g

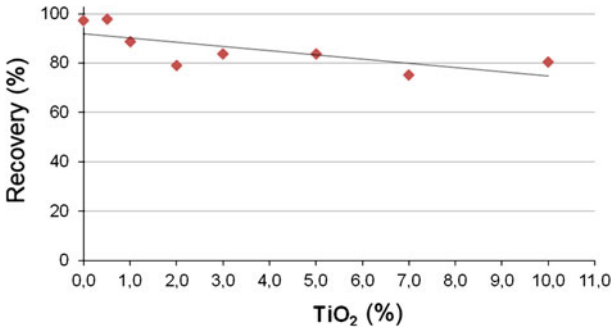

Fig. 8 Recovery by DMTA analysis of the synthesized materials

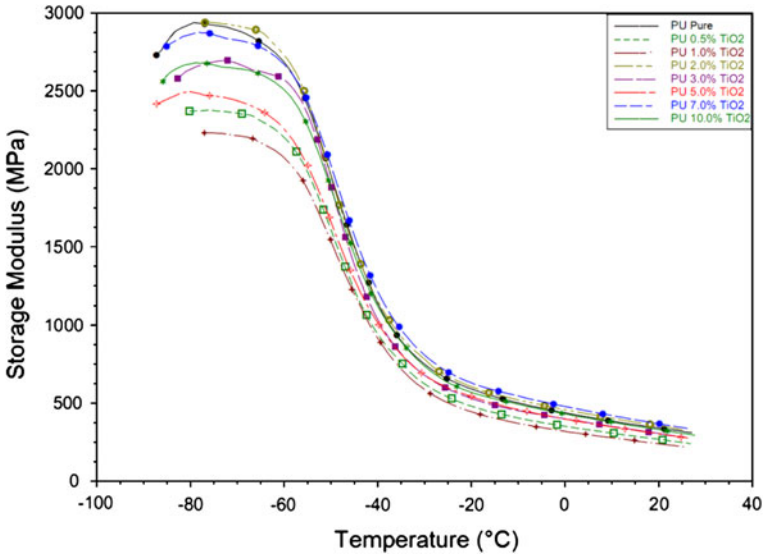

Fig. 9 Storage modulus of nanocomposites synthesized with 0.0, 0.5, 1.0, 2.0, 3.0, 5.0, 7.0, and 10.0 % TiO_2

value indicates a reduction in the mobility of polymer chains due to the interactions between the polymer and the nanofiller [36]. The decrease in the molecular weight with the increase of the filler content probably contributed to the small variation in T_g values (Figs. 4 and 5).

The results of stress–strain tests can be seen in Fig. 6. The nanocomposites with 0.5 and 1.0 % of TiO_2 behaved slightly less than pure PU film, but the materials prepared with 2.0, 3.0, and 5.0 % of TiO_2 had higher values of stress to a same deformation when compared to pure PU. Materials with 7.0 and 10.0 % of filler became more fragile, probably by the increase of the crosslinks formed between the nanoparticles and the polymer matrix. A higher agglomeration of the fillers could also cause many stress points in the polymer matrix, resulting in lower mechanical properties, as noted by Zhang et al. [37].

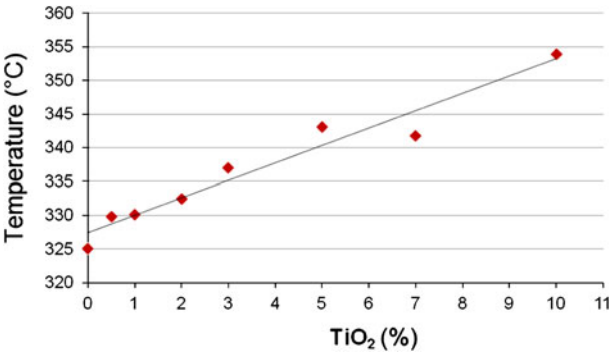

Fig. 10 Onset temperature of degradation in function of TiO_2(%)

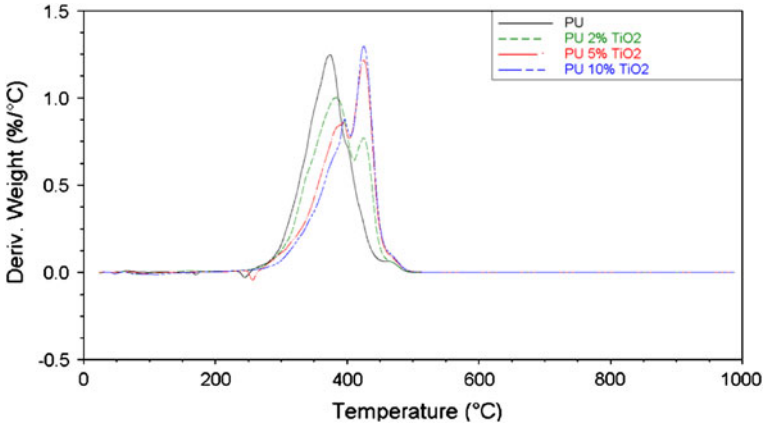

Fig. 11 DTGA curves (%/ °C) versus temperature of the PU and the nanocomposites of PU and TiO_2 [2, 5, 10 % (w/w)]

For the nanocomposites with 0.5 and 1.0 % TiO_2, the Young's moduli were practically the same as the pure PU, suggesting that the elastic behavior was not affected by filler incorporation. The nanocomposites with 2.0, 3.0, and 5.0 % had higher values, and the material with 2.0 % of TiO_2 presented a Young's modulus about 30 % higher compared to the pure polymer (Fig. 7). Due to the films fragility, the Young's moduli of the materials with 7.0 and 10.0 % of filler were not calculated. It can be seen from Fig. 10 that the materials have mechanical properties maximized by the nanofiller addition until 5.0 % of reinforcement; when a larger amount of TiO_2 was added the values decreased, probably by the formation of agglomeration focus, which results in significant increase in the interaction filler/filler making the material britle [36].

Sabzi et al. [27] and Mirabedini el al. [31] have reached, for TiO_2 nanocomposites, an increase of 49 and 40 % in the Young's modulus when compared to the pure polymer. Both works used previously treated TiO_2 and the nanocomposites were prepared by a solvent mixture. Our results showed that an increase of 30 % in

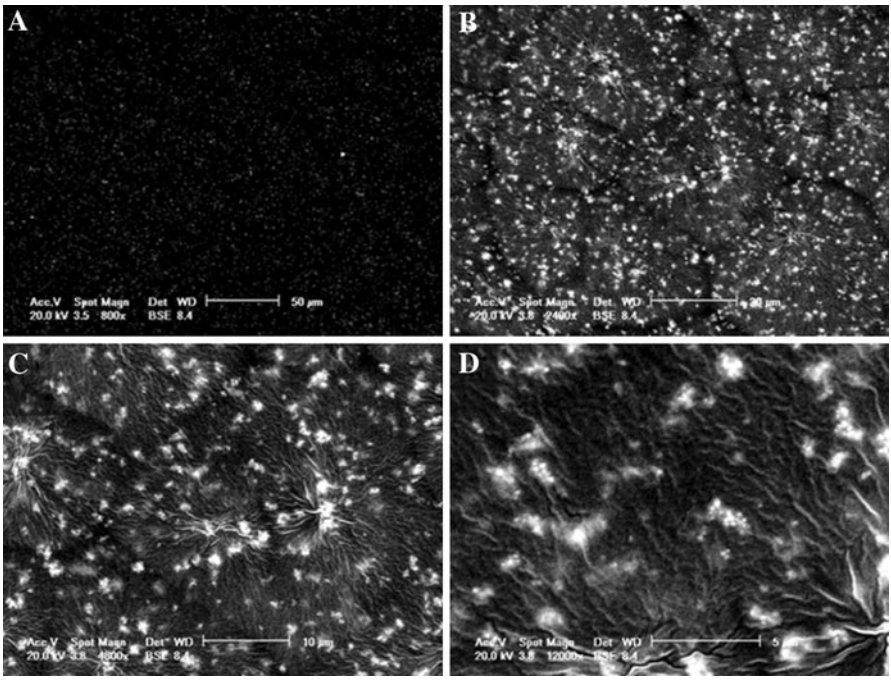

Fig. 12 Micrographs, mode BSE, of the nanocomposite with 5.0 % of TiO_2 at magnifications of: **a** ×800, **b** ×2400, **c** ×4800, **d** ×12000

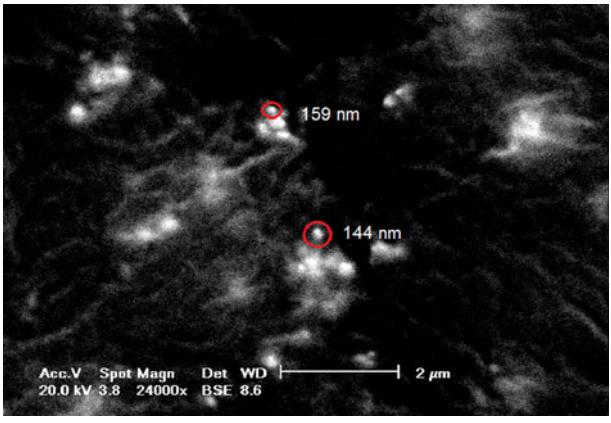

Fig. 13 Micrographs, mode BSE, of the nanocomposite with 7.0 % TiO_2 with magnification of ×2,400

Young's modulus of the nanocomposite with respect to the PU pure can be achieved using TiO_2 not exposed to pretreatment before in situ polymerization.

The creep-recovery tests in the DMTA showed that the increase of filler in the polymeric matrix leads to a gradual decrease on the recovery percent after deformation (Fig. 8).

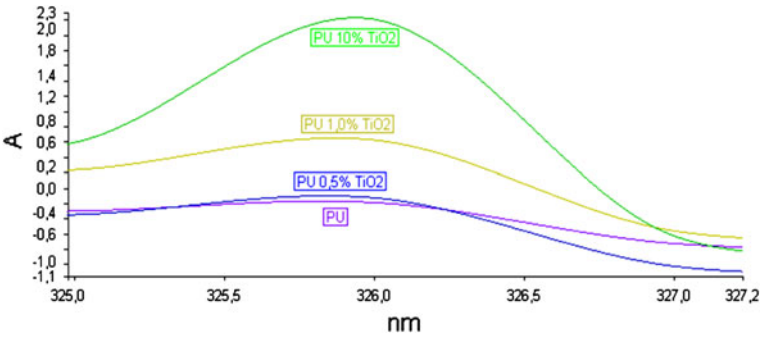

Fig. 14 Effect of the TiO_2 content on UV–Vis absorption of the composite materials

The interaction between the polymer and the charge could restrict the movement of the polymer chains resulting in a reduction in the elastic behavior of the material making it more rigid and thus less elastomeric when compared to pure polymer. The nanocomposite with 7.0 % of TiO_2 showed the lowest recovery (75 %) when compared to pure polymer which recovered 97 % of the deformation.

The Fig. 9 shows the variation of the storage modulus (E') as a function of temperature. There is a decline with the increasing of the temperature.

A slight increase in storage modulus occurs at a temperature of 0 °C (the rubbery region) for the material with 2 % TiO_2 (457.3 MPa) and 7 % of TiO_2 (477.2 MPa) as compared to pure PU (436, 6 MPa). At −65 °C (glass region), the nanocomposite with 2 % TiO_2 (2890 MPa) showed slightly higher value of storage modulus when compared to the pure PU (2826 MPa) (Fig. 12). This is an advantage of a nanocomposite which is capable of maintaining high modulus even at temperatures above T_g (the rubbery region). Generally, the addition of inorganic fillers and pigments in polymers increases the storage modulus in the rubbery region and not in the glassy region [27].

The TGA analysis showed a significant increase in degradation temperature of the nanocomposites evidencing that the thermal resistance increased with the increase in the amount of filler added (Fig. 10).

The degradation temperature of the pure polymer was the lowest, showing a value close to 325 °C, and the temperature of the nanocomposite with 10.0 % of TiO_2 was the highest, which reached approximately 354 °C, showing a variation in the degradation temperature of about 29 °C. Analyzing the DTG curves (%/°C), Fig. 11, it was seen that the increase of a second peak related to the increase of TiO_2 content; it occurred, probably, due to the formation of a network structure by the surface hydroxyl groups of the nanofiller through hydrogen bonding which acts as a thermal insulator and mass transport barrier to the volatile products generated during the decomposition and thus increases the degradation temperatures [38].

The Fig. 12 shows that a relatively even distribution of the filler can be observed in polymeric matrix, important to maximize the mechanical properties throughout the polymer matrix and not just punctually. In Fig. 13, it is possible to see small agglomeration points of TiO_2, as well as that some of these clusters are composed of smaller particles with diameters in the nanometer range.

The analysis by SEM showed that there were some focuses of clusters formed by the TiO_2. These sites can be considered as weak points in the material. The UV–Vis spectroscopy corroborates the filler incorporation. Figure 14 shows the spectra for PU and for composites with 0.5, 1, and 10 % of TiO_2. It is clear that the increasing in the TiO_2 particles content augments the absorption in the UV wavelength region.

Conclusion

Based on the obtained results we had concluded that the nanocomposites synthesized by in situ polymerization presented, in general, thermal properties (degradation temperature) and mechanical properties higher than the pure polymer. Despite showing a degradation temperature lower than the materials with higher amounts of TiO_2, the additions of 2.0, 3.0, and 5.0 % showed to be the most efficient in tensile tests. The increase in the T_g value indicates that there was a decrease in the mobility of polymer chains due to the action of the filler. This reduction can also be seen by the results of the creep-recovery test, which showed that the percentage of recovery after deformation is related with the major amount of the filler. There was, also, a slight increase in storage modulus in the rubbery region (above the T_g) as compared to the vitreous region (below the T_g). The stress–strain tests showed that the material with 2 % of TiO_2 improved in its Young's modulus when compared to the pure polymer, indicating an increase in the mechanical strength. The SEM analysis showed that even with some agglomeration points, it was possible to achieve efficient nanofiller dispersion without any treatment of TiO_2, which leads to a reduction in the process cost.

Acknowledgments The authors thank PRONEX/Fundação de Amparo a Pesquisa do Estado do RS/Conselho Nacional de Pesquisa e desenvolvimento-CNPq and Agência Brasileira de Inovação for research grant. SE thanks CNPq for scholarship in technical development productivity. CC thanks Coordenação de Aperfeiçoamento de Pessoal de Nível Superior for PNPD post-doc fellowship.

References

1. Malíková M, Rychlý J, Matisová-Rychlá L, Csomorová K, Janigová I, Wilde H-W (2010) Assessing the progress of degradation in polyurethanes by chemilum inescence. I. Unstabilised polyurethane films. Polym Degrad Stab 95:2367–2375. doi:10.1016/j.polymdegradstab.2010.08.016
2. Lu Y, Tighzert L, Berzin F, Rondot S (2005) Innovative plasticized starch films modified with waterborne polyurethane from renewable resources. Carbohydr Polym 61:174–182. doi:10.1016/j.carbpol.2005.04.013
3. Thomas PS, Thomas S, Bandyopadhyay S, Wurm A, Schick C (2008) Polystyrene/calcium phosphate nanocomposites: dynamic mechanical and differential scanning calorimetric studies. Compos Sci Technol 68:3220–3229. doi:10.1016/j.compscitech.2008.08.008
4. Ray SS, Yamada K, Okamoto M, Ueda K (2002) Polylactide-layered silicate nanocomposite: a novel biodegradable material. Nano Lett 2:1093–1096. doi:10.1021/nl0202152
5. Zia KM, Bhatti HN, Bhatti IA (2007) Methods for polyurethane and polyurethane composites, recycling and recovery: a review. React Funct Polym 67:675–692. doi:10.1016/j.reactfunctpolym.2007.05.004
6. Khalil M, Saeed S, Ahmad Z (2008) Mechanical and thermal properties of polyimide/silica hybrids with imide-modified silica network structures. J Appl Polym Sci 107:1257–1268. doi:10.1002/app.27149

7. Vladimirov V, Betchev C, Vassiliou A, Papageorgiou G, Bikiaris D (2006) Dynamic mechanical and morphological studies of isotactic polypropylene/fumed silica nanocomposites with enhanced gas barrier properties. Compos Sci Technol 66:2935–2944. doi:10.1016/j.compscitech.2006.02.010
8. Pavlidou S, Papaspyrides CD (2008) A review on polymer-layered silicate nanocomposites. Prog Polym Sci 33:1119–1198. doi:10.1016/j.progpolymsci.2008.07.008
9. Chen Y, Wang R, Zhou J, Fan H, Shi B (2011) Membrane formation temperature-dependent gas transport through thermo-sensitive polyurethane containing in situ-generated TiO_2 nanoparticles. Polymer 52:1856–1867. doi:10.1016/j.polymer.2011.02.021
10. Esteves ACC, Barros-Timmons A, Trindade T (2004) Nanocompósitos de Matriz Polimérica: estratégias de Síntese de Materiais Híbridos. Quim Nova 27:798–806
11. Yang K, Yang Q, Li G, Sun Y, Feng D (2006) Morphology and mechanical properties of polypropylene/calcium carbonate nanocomposites. Mater Lett 60:805–809. doi:10.1016/j.matlet.2005.10.020
12. Oriakhi CO (2000) Polymer nanocomposition approach to advanced materials. J Chem Educ 77:1138–1146. doi:10.1021/ed077p1138
13. Gao X, Zhou B, Guo Y, Zhu Y, Chen X, Zheng Y, Gao W, Ma X, Wang Z (2010) Synthesis and characterization of well-dispersed polyurethane/$CaCO_3$ nanocomposites. Colloids Surf A 371:1–7. doi:10.1016/j.colsurfa.2010.08.036
14. Reyes-Coronado D, Rodríguez-Gattorno G, Espinosa-Pesqueira ME, Cab C, Coss R, Oskam G (2008) Phase-pure TiO_2 nanoparticles: anatase, brookite and rutile. Nanotechnology 19:10. doi:10.1088/0957-4484/19/14/145605
15. Bavykin DV, Friedrich JM, Walsh FC (2006) Protonated titanates and TiO_2 nanostructured materials: synthesis, properties, and applications. Adv Mater 18:2807–2824. doi:10.1002/adma.200502696
16. Reijnders L (2009) The release of TiO_2 and SiO_2 nanoparticles from nanocomposites. Polym Degrad Stab 94:873–876. doi:10.1016/j.polymdegradstab.2009.02.005
17. Imai Y, Terahara A, Hakuta Y, Matsui K, Hayashi H, Ueno N (2009) Transparent poly(bisphenol A carbonate)-based nanocomposites with high refractive index nanoparticles. Eur Polym J 45:630–638. doi:10.1016/j.eurpolymj.2008.12.031
18. Mahmoudian MR, Basirun WJ, Alias Y (2011) Synthesis of polypyrrole/Ni-doped TiO_2 nanocomposites (NCs) as a protective pigment in organic coating. Prog Org Coat 71:56–64. doi:10.1016/j.porgcoat.2010.12.010
19. Xian G, Walter R, Haupert F (2006) Friction and wear of epoxy/TiO_2 nanocomposites: influence of additional short carbon fibers, aramid and PTFE particles. Compos Sci Technol 66:3199–3209. doi:10.1016/j.compscitech.2005.02.022
20. Mihailovic D, Saponjic Z, Radoicic M, Radetic T, Jovancic P, Nedeljkovic J, Radetic M (2010) Functionalization of polyester fabrics with alginates and TiO_2 nanoparticles. Carbohydr Polym 79:526–532. doi:10.1016/j.carbpol.2009.08.036
21. Jiang X, Tian X, Gu J, Huang D, Yang Y (2011) Cotton fabric coated with nano TiO_2-acrylate copolymer for photocatalytic self-cleaning by in situ suspension polymerization. Appl Surf Sci 257:8451–8456
22. Patra N, Salerno M, Malerba M, Cozzoli PD, Athanassiou A (2011) Improvement of thermal stability of poly(methyl methacrylate) by incorporation of colloidal TiO_2 nanorods. Polym Degrad Stab 96:1377–1381. doi:10.1016/j.polymdegradstab.2011.03.020
23. Shi Y, Mu L, Feng X, Lu X (2011) The tribological behavior of nanometer and micrometer TiO_2 particle-filled polytetrafluoroethylene/polyimide. Mater Des 32:964–970. doi:10.1016/j.matdes.2010.07.013
24. Liaw W-C, Chen K-P (2007) Preparation and characterization of poly(imide siloxane) (PIS)/titania(TiO_2) hybrid nanocomposites by sol–gel processes. Eur Polym J 43:2265–2278. doi:10.1016/j.eurpolymj.2007.01.015
25. Song M, Pan C, Li J, Zhang R, Wang X, Gu Z (2008) Blends of TiO_2 nanoparticles and poly(*N*-isopropylacrylamide)-*co*-polystyrene nanofibers as a means to promote the biorecognition of an anticancer drug. Talanta 75:1035–1040. doi:10.1016/j.talanta.2008.01.005
26. Zhang L, Liu P, Su Z (2006) Preparation of PANI-TiO_2 nanocomposites and their solid-phase photocatalytic degradation. Polym Degrad Stab 91:2213–2219
27. Sabzi M, Mirabedini SM, Zohuriaan-Mehr J, Atai M (2009) Surface modification of TiO_2 nanoparticles with silane coupling agent and investigation of its effect on the properties of polyurethane composite coating. Prog Org Coat 65:222–228. doi:10.1016/j.porgcoat.2008

28. Che X-C, Jin Y-Z, Lee Y-S (2010) Preparation of nano-TiO_2/polyurethane emulsions via in situ RAFT polymerization. Prog Org Coat 69:534–538. doi:10.1016/j.porgcoat.2010.09.013
29. Chen J, Zhou Y, Nan Q, Ye X, Sun Y, Zhang F, Wang Z (2007) Preparation and properties of optically active polyurethane/TiO_2 nanocomposites derived from optically pure 1,1′-binaphthyl. Eur Polym J 43:4151–4159. doi:10.1016/j.eurpolymj.2007.07.006
30. Kasanen J, Suvanto M, Pakkanen TT (2011) UV stability of polyurethane binding agent on multilayer photocatalytic TiO_2 coating. Polym Test 30:381–389. doi:10.1016/j.polymertesting.2011.02.006
31. Mirabedini SM, Sabzi M, Zoguriaan-Mehr J, Atai M, Behzadnasab M (2011) Weathering performance of the polyurethane nanocomposite coatings containing silane treated TiO_2 nanoparticles. Appl Surf Sci 257:4196–4203. doi:10.1016/j.apsusc.2010.12.020
32. Chen J, Zhou Y, Nan Q, Sun Y, Ye X, Wang Z (2007) Synthesis, characterization and infrared emissivity study of polyurethane/TiO_2 nanocomposites. Appl Surf Sci 253:9154–9158. doi:10.1016/j.apsusc.2007.05.046
33. Zheng J, Ozisik R, Siegel RW (2005) Disruption of self-assembly and altered mechanical behavior in polyurethane/zinc oxides nanocomposites. Polymer 46:10873–10882. doi:10.1016/j.polymer.2005.08.082
34. Polizos G, Tuncer E, Agapov AL, Stevens D, Sokolov AP, Kidder MK, Jacobs JD, Koerner H, Vaia RA, More KL, Sauers I (2012) Effect of polymer–nanoparticle interactions on the glass transition dynamics and the conductivity mechanism in polyurethane titanium dioxide nanocomposites. Polymer 53:595–603. doi:10.1016/j.polymer.2011.11.050
35. Paiva JMF, Mayer S, Rezende MC, Cândido GM (2006) Avaliação da temperatura de transição vítrea de compósitos poliméricos reparados de uso aeronáutico. Polímeros 16:79–87
36. Zhang SW, Liu R, Jiang JQ, Yang C, Chen M, Liu XY (2011) Facile synthesis of waterborne UV-curable polyurethane/silica nanocomposites and morphology, physical properties of its nanostructured films. Prog Org Coat 70:1–8. doi:10.1016/j.porgcoat.2010.09.005
37. Ma X-Y, Zang W-D (2009) Effects of flower-like ZnO nanowhiskers on the mechanical, thermal and antibacterial properties of waterborne polyurethane. Polym Degrad Stab 94:1103–1109. doi:10.1016/j.polymdegradstab.2009.03.024
38. Mishra AK, Mishra RS, Narayan R, Raju KVSN (2010) Effect of nano ZnO on the phase mixing of polyurethane hybrid dispersions. Prog Org Coat 67:405–413. doi:10.1016/j.porgcoat.2009.12.008